



## A family of Finslerian space-time obeying MIT-bag equation of state

Ksh. Newton Singh, M. V. Mandke, Anil K. Aria

Department of Physics, National Defence Academy, Khadakwasla, Pune, Maharashtra-411023, India

Received 02nd March 2021, Accepted 1<sup>st</sup> April 2021

### Abstract

*In this article, a family of Finslerian space times describing stellar configurations obeying MIT-bag equation of state (EoS) is presented. Here we have adopted a new method of solving the field equation by assuming one of the metric potential along with the MIT-bag EoS and solve for the other metric potential. We have also assumed an anisotropic matter distribution which described physically possible matters since the EoS parameter  $\omega_r$  and  $\omega_t$  are less than unity. These solutions obey causality ( $v_r, v_t \leq 1$ ) and stability condition ( $0 \leq |v_t^2 - v_r^2| \leq 1$ ). These solutions are well-behaved at the interior except at the centre  $r = 0$  since it contains singularity. The properties of the stellar configurations described by these solutions are solely depends on parameter  $n$ . For small values of  $n$  corresponds to softer EoSs that yields less massive and smaller configurations, however, larger values of  $n$  gives more denser, massive and bigger configurations where the EoSs are stiffer. It has been observed that the anisotropy is more for smaller values of  $n$  than bigger values. Above all, these solutions satisfy all the energy conditions implying that these can represent physical matters. Two models of well-known compact stars are also presented and indeed the calculated values of masses and radii are well match with the observed ones.*

**Keywords:** Modified theory of gravity, Finsler geometry, Compact stars, Equation of state, Anisotropy

Copy Right, IJRRAS, 2021. All Rights Reserved.

### Introduction

In the past few decades, researchers are more attracting towards the formation, structure and evolution of compact stars. Now it is well-known that compact stars like neutron stars (NS) may form through the process of type-Ia and type-II supernovae. It is still uncertain about the exact matter composition of NS. Indeed, we are able to understand some of the possible matter that may present such as free neutrons in superfluid state, free protons in superconducting state with some electrons and solid nuclei. Many theories have been proposed that asymptotically free quarks may also exist at the core of NS.

dimension by adding quadratic terms on Riemann tensor in Einstein-Hilbert action. The reason why we want to modify Einstein-Hilbert action is that the higher order derivative curvature terms makes non-zero contribution to the dynamics. Jhingan & Ghosh (2010) studied spherically symmetric inhomogeneous dust and

Pions and Kaons are also physically favoured to exist in condensate state.

Despite of their internal structure, general relativist are trying to construct solutions of Einstein's field equations to model such compact stars. Many solutions has been discovered, however, only few of them are appreciated physically (Delgaty & Lake 1998; Singh *et al.* 2015; Singh & Pant 2015a; Bhar 2015a,b). Other than the Einsteinian gravity, many researchers are also devoted to alternative or modified theories of gravity.

Gauss-Bonnet (GB) extended the Einstein's theory of gravity to fifth

null dust in GB gravity with non-zero coupling constant modifies the causal structure of black holes compared to the standard 5-D general relativistic case. The study of Vaidya radiating black-holes in GB gravity has revealed that the location of the horizons is changed as compared to the standard 4-D gravity (Ghosh & Deshkar 2008). The Schwarzschild interior solution to describe a uniform density sphere in higher dimensions requires a necessary and sufficient condition that the number of dimensions should be at least four i.e.  $d \geq 4$  (Dadhich *et al.* 2010). Bhar *et al.* (2017) have also shown that the

### Correspondence Author

Ksh. Newton Singh, Department of Physics, National Defence Academy, Khadakwasla, Pune, Maharashtra-411023, India

central density and pressure are higher in GB-gravity than the 5-D Einstein gravity.

The higher order theory of gravity was proposed by Lovelock (1971, 1972) generalizing the Einstein's gravity to  $N^{th}$ -order gravity in  $d$ -dimensions. The Einstein-Hilbert Lagrangian was now generalized into Lanczos-Lovelock Lagrangian that includes homogeneous polynomials of degree  $N$  in Riemann curvature. Remarkable results of Lovelock gravity are those includes cosmological term  $N = 0$ , Einstein gravity for  $N = 1$  and quadratic GB for  $N = 2$ , and so on. It is shown that black hole in Lovelock gravity possesses thermodynamical universality i.e. the temperature and entropy bear the same relation to the event horizon radius as the Einstein black hole in 3-D and 4-D irrespective of the Lovelock order  $N$  (Dadhich *et al.* 2013).

Researchers are also eager to quantize the gravity so that all the four fundamental forces can be unify into a single theory (The Theory of Everything). However, it is still a big and open problem on how to quantize gravity. However, GR is not renormalizable and hence can't be quantized. Indeed, Utiyama & De-Witt (1962)

$$S_{FR} = \frac{1}{16\pi} \int f_0 R^{1+v_{tg}^2} \sqrt{-g} dx^4 \quad (3)$$

i.e.  $f(R) = f_0 R^{1+v_{tg}^2}$ , where  $f_0$  is a positive constant and  $v_{tg}$  is the tangential velocity of the test particles.

Many authors have also used the  $f(R)$ -gravity formalism in describing astrophysical object such as compact stars (Zubair & Abbas 2016; Capozziello *et al.* 2011, 2012). Another promising alternative theory of gravity was proposed by Finsler (Bao *et al.* 2000) now known as Finslerian gravity. Here the Riemann geometry is a special case where the four-velocity vector is treated as independent variable. The first self-consistent Finsler geometry was formulated by Cartan (1934). Further, Cartan  $d$ -connected were first introduced by Horvath (1950) and many researchers start using Finsler gravity as applications in physics (Vacaru 2010, 2012; Schreck 2015).

Even though, it is not an easy task to solve field equations in Finsler geometry exactly. Vacaru (1997, 1996) derived the Finsler gravity and locally anisotropic spinors in the low energy limits of superstring/supergravity theories with N-connection structure where the velocity type coordinates are treated as extra-dimensions. Anholonomic frame deformation method in

and Stelle (1977) shows that gravity is possible to renormalize if one includes higher order curvature terms in Einstein-Hilbert action. Hence, one of the most promising theory of gravity that includes higher order curvature terms is  $f(R)$ -gravity. In  $f(R)$ -gravity the Einstein-Hilbert action i.e.

$$S_{EH} = \frac{1}{16\pi} \int dx^4 \sqrt{-g} R \quad (1)$$

is modified into more general form as

$$S_{FR} = \frac{1}{16\pi} \int dx^4 \sqrt{-g} f(R) \quad (2)$$

where  $g$  is the determinant of the metric tensor and  $R$  is the Ricci scalar. The reason why we choose only  $f(R)$  is because of its simplicity and it also avoids Ostrogradski instability (Woodard 2007). Using the formalism of  $f(R)$ -gravity Bohmer *et al.* (2008) shown the motion of test particles around galaxies i.e. rotational curves of galaxies can be explain without the inclusion of hypothetical dark matter. They also found that the form of  $f(R)$  that described the dynamics of galaxies as

Finsler geometry was used to construct generic off-diagonal exact solutions in various modified theories of gravity (Vacaru 2012; Stavrinos & Vacaru 2013; Rajpoot & Vacaru 2015). Recently, Rahaman *et al.* (2015, 2016) have used Finsler geometry to described compact stars structure and worm holes. By assuming a relationship between mass function and a metric coefficient along with a linear EoS, they discovered a new exact solution to model compact stars.

In this article, we have adopted a new method in the Finsler geometry to solve the field equations by assuming one of the metric potential with the MIT-bag EoS. These new solutions describe matter distributions with anisotropy in pressure. The article is organized as follows: sect. 2 discussed Einstein field equations in Finsler geometry, sect. 3 deals with the method of generating the new solutions, sect. 4 elaborate the properties of these new solutions, in sect. 5 the matching of interior and exterior spacetime is performed at the boundary, sect. 6 is devoted to equilibrium and stability analysis via various methods and last sect. 7 discussed the physical applications of these new solutions.

### Einstein field equations in Finslerian geometry

The Finslerian geometry is constructed from Finsler structure  $F$  which is defined as

$$(x, \mu y) = \mu F(x, y) \quad \forall \mu > 0. \quad (4)$$

Here  $x \in M$  represents position and  $y = dx/dt$ , the velocity. The metric describing Finslerian geometry is given as

The geodesic equation in Finsler manifold is

The geodesic equation in Finsler manifold is expressed as

$$\frac{d^2 x^\mu}{dt^2} + 2G^\mu = 0 \quad (6)$$

where  $G^\mu$  is called the geodesic spray coefficients defined as

$$G^\mu = \frac{1}{4} g^{\mu\nu} \left( \frac{\partial^2 F^2}{\partial x^\lambda \partial y^\nu} y^\lambda - \frac{\partial F^2}{\partial x^\nu} \right) \quad (7)$$

The Ricci scalar in Finsler geometry is written

$$R \equiv R^\mu_\nu = \frac{1}{F^2} \left( 2 \frac{\partial G^\mu}{\partial x^\mu} - y^\lambda \frac{\partial^2 G^\mu}{\partial x^\lambda \partial y^\mu} + 2G^\lambda \frac{\partial^2 G^\mu}{\partial x^\lambda \partial y^\mu} - \frac{\partial G^\mu}{\partial y^\lambda} \frac{\partial G^\lambda}{\partial y^\mu} \right) \quad (8)$$

$$R^\mu_\nu = \frac{1}{F^2} R^\mu_{\lambda\nu p} y^\lambda y^p \quad (9)$$

Here  $R^\mu_{\lambda\nu p}$  depends on connections and  $R^\mu_\nu$

depends only on the Finsler structure  $F$ .

Assuming the Finsler structure of the form (Li & Chang 2014)

$$F^2 = B(r) y^t y^t - A(r) y^r y^r - r^2 \bar{F}^2 \left( \theta, \phi, y^\theta y^\phi \right) \quad (10)$$

The Finsler metric are given below

$$g^{\mu\nu} = \text{diag} \left( B, -A, -r^2 \bar{g}_{ij} \right) \quad (11)$$

$$g^{\mu\nu} = \text{diag} \left( B^{-1}, -A, -r^{-2} \bar{g}_{ij} \right) \quad (12)$$

where  $\bar{g}_{ij}$  are derived from  $\bar{F}$  and  $(\theta, \phi) \equiv$

$(i, j)$ .

We can now able to write the Einstein's tensor in Finsler geometry as

$$g_{\mu\nu} \equiv \frac{\partial}{\partial y^\mu \partial y^\nu} \left( \frac{1}{2} F^2 \right) \quad (5)$$

expressed as

The components of geodesic spray coefficient becomes

$$G^t = \frac{B'}{2B} y^t y^r \quad (13)$$

$$G^r = \frac{A'}{4A} y^r y^r + \frac{B'}{4A} y^t y^t - \frac{r}{2A} \bar{F}^2 \quad (14)$$

$$G^\theta = \frac{1}{r} y^\theta y^r + \bar{G}^\theta \quad (15)$$

$$G^\phi = \frac{1}{r} y^\phi y^r + \bar{G}^\phi \quad (16)$$

where the prime represents differentiation with respect to  $r$  and the  $\bar{G}$  is the geodesic spray coefficients derived by  $\bar{F}$ . Substituting (13)-(16) to (8) we the expression of Ricci scalar as

$$F^2 R = \left[ \frac{B''}{2A} - \frac{B'}{4A} \left( \frac{A'}{A} + \frac{B'}{B} \right) + \frac{B'}{rA} \right] y^t y^t + \left[ -\frac{B''}{2B} + \frac{B'}{4B} \left( \frac{A'}{A} + \frac{B'}{B} \right) + \frac{A'}{rA} \right] y^r y^r + \left[ \bar{R} - \frac{1}{A} + \frac{r}{2A} \left( \frac{A'}{A} + \frac{B'}{B} \right) \right] \bar{F}^2 \quad (17)$$

provided  $\bar{R}$  is the Ricci scalar correspond to  $\bar{F}$ . Akbar-Zadeh (1988) first introduced the notion of Ricci tensor in the Finsler geometry as

$$R_{\mu\nu} = \frac{\partial^2}{\partial y^\mu \partial y^\nu} \left( \frac{1}{2} F^2 R \right) \quad (18)$$

The scalar curvature in the Finsler geometry is defined as  $S = g^{\mu\nu} R_{\mu\nu}$ .

Now the modified Einstein's tensor is given by

$$G_{\mu\nu} \equiv R_{\mu\nu} - \frac{1}{2} g_{\mu\nu} S \quad (19)$$

The covariant conservation of  $G_{\mu\nu}$  in Finsler geometry i.e.  $G^\mu_{\nu;\mu} = 0$  was proved by Li & Chang (2014).

$$G_t^t = \frac{A'}{rA^2} - \frac{1}{r^2A} + \frac{\lambda}{r^2} \quad (20)$$

$$G_r^r = -\frac{B'}{rAB} - \frac{1}{r^2A} + \frac{\lambda}{r^2} \quad (21)$$

$$G_\theta^\theta = G_\phi^\phi = -\frac{B''}{2AB} - \frac{B'}{2rAB} + \frac{A'}{2rA^2} + \frac{B'}{4AB} \left( \frac{A'}{A} + \frac{B'}{B} \right) \quad (22)$$

Finally, we can write the field equations in Finsler space-time as

$$G_v^\mu = 8\pi_F T_v^\mu \quad (23)$$

with  $T_v^\mu$  is the energy-momentum tensor and  $4\pi_F$  is expressing the volume of  $\bar{F}$  in the field equation.

Assuming a matter distribution with anisotropy in pressure, the form of energy-momentum tensor can be written as

$$T_\zeta^\mu = \rho v^\mu v_\zeta + p_r \chi_\zeta^\mu \chi^\mu + p_t \left( v^\mu v_\zeta - \chi_\zeta^\mu \chi^\mu + g_\zeta^\mu \right) \quad (24)$$

where  $v^\mu v_\mu = -\chi^\mu \chi_\mu = 1$ ,  $p_r$  and  $p_t$  denote radial and transverse pressures respectively,  $\rho$  is the density of the fluid distribution,  $v^\mu$  the four velocity and  $\chi^\mu$  is the unit space-like vector in the radial direction.

On using the energy-momentum tensor in (24) along with the field equation (23) we get

$$8\pi_F \rho(r) = \frac{A'}{rA^2} - \frac{1}{r^2A} + \frac{\lambda}{r^2} \quad (25)$$

$$8\pi_F p_r(r) = \frac{B'}{rAB} + \frac{1}{r^2A} - \frac{\lambda}{r^2} \quad (26)$$

$$8\pi_F p_t(r) = \frac{B''}{2AB} + \frac{B'}{2rAB} - \frac{A'}{2rA^2} - \frac{B'}{4AB} \left( \frac{A'}{A} + \frac{B'}{B} \right) \quad (27)$$

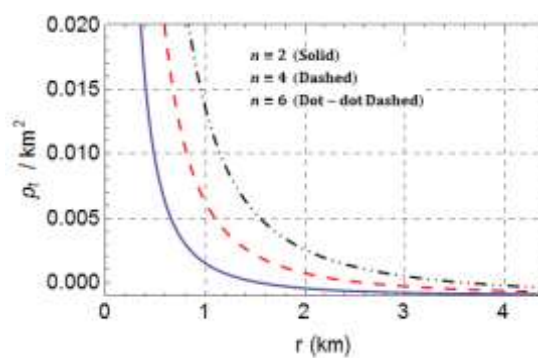
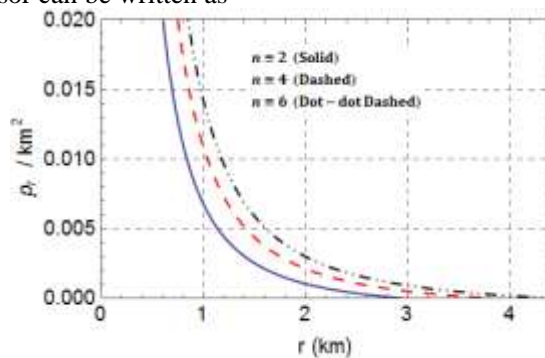


Figure 1. Variation of  $p_r$  and  $p_t$  with radial coordinate  $r$  for  $c = 0.001, \alpha = 0.7, \beta = 0.001, \lambda = 101$  and  $k = 0.01$ .

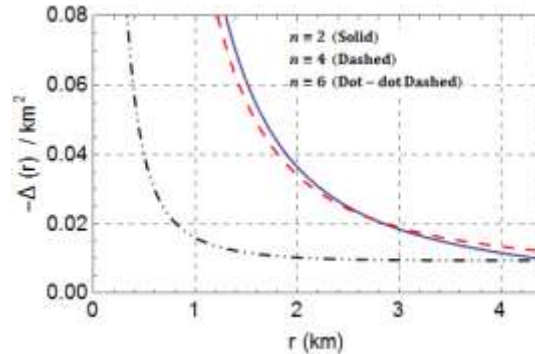
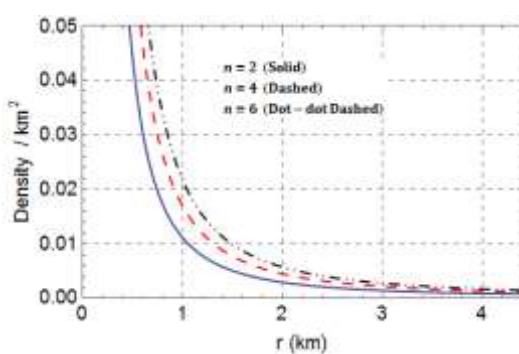


Figure 2. Variation of  $\rho$  and  $-\Delta$  with radial coordinate  $r$  for  $c = 0.001, \alpha = 0.7, \beta = 0.001, \lambda = 101$  and  $k = 0.01$ .

### Generating a new family of solutions in Finsler geometry

Rahaman *et al.* (2015) have generated a new solution in Finsler space-time by assuming a particular form of mass function  $m(r)$  which was linked with the metric  $A$  as  $A^{-1} = \lambda - 2Gm(r)/r$ . However, in this paper we are using a new approach by assuming one of the metric potential. Here we have assumed  $A(r)$  in the background of MIT-bag EoS

$$A(r) = (\lambda + cr^2)^n \quad \forall n > 1 \quad (28)$$

$$p(r) = \alpha\rho(r) - \beta \quad (29)$$

where  $n$  is a real number,  $c$  is a constant which is determined from the boundary conditions.

On using (25) and (26) in (29) we get

$$-\frac{\alpha A'}{A^2 r} + \frac{B'}{ArB} + \frac{\alpha + 1}{Ar^2} + 8\pi_F \beta - \frac{(\alpha + 1)\lambda}{r^2} = 0 \quad (30)$$

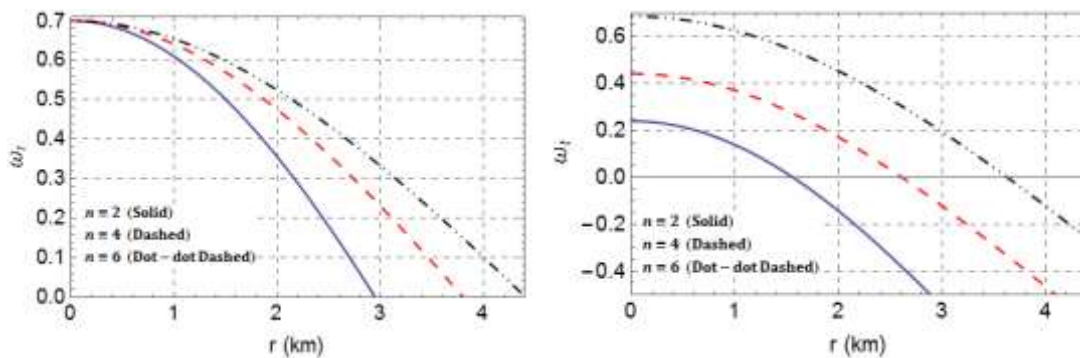


Figure 3. Variation of  $\omega_r$  and  $\omega_t$  with radial coordinate  $r$  for  $c = 0.001, \alpha = 0.7, \beta = 0.001, \lambda = 101$  and  $k = 0.01$ .

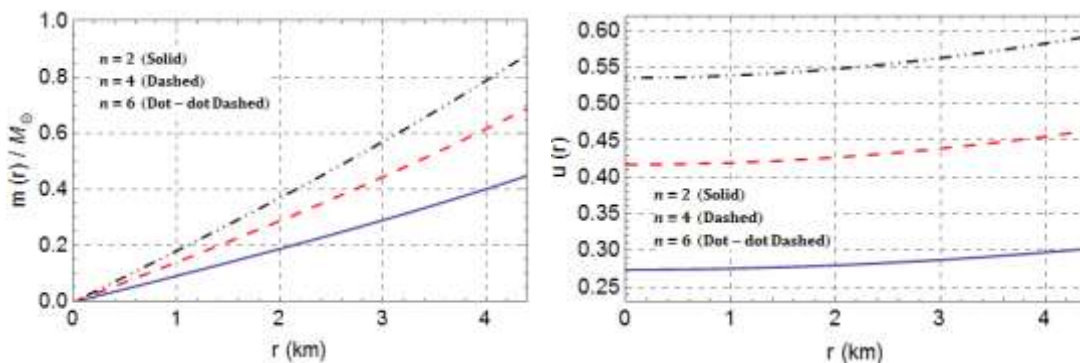


Figure 4. Variation of  $m(r)/M_\odot$  and  $u(r)$  with radial coordinate  $r$  for  $c = 0.001, \alpha = 0.7, \beta = 0.001, \lambda = 101$  and  $k = 0.01$ .

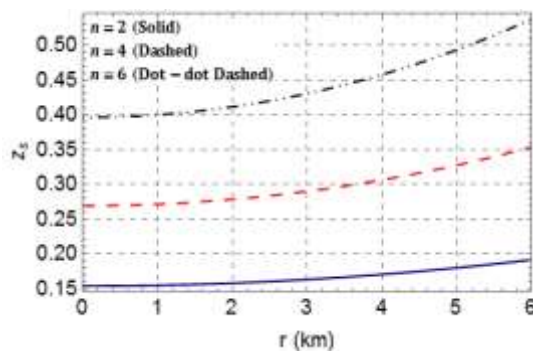
Putting (28) in (30) we get

$$B(r) = \frac{k}{r^{\alpha+1}} (cr^2 + \lambda)^{\alpha n} \exp\left[\frac{1}{2}\right] (cr^2 + \lambda)^n$$

$$\left\{ -\frac{8\pi_F \beta}{c(n+1)} \left[ cr^2 + \lambda - \lambda \left( \frac{cr^2}{\lambda} + 1 \right)^{-n} \right] \right.$$

$$\left. + \frac{(\alpha+1)\lambda}{n} \left( \frac{\lambda}{cr^2} + 1 \right)^{-n} \right\}$$

$${}_2F_1 \left[ -n, -n; 1-n; -\frac{\lambda}{cr^2} \right] \quad (31)$$



where  ${}_2F_1$  is the usual hypergeometric function defined as

$${}_2F_1[a, b; c; z] = \sum_{i=0}^{\infty} \frac{(a)_i (b)_i}{(c)_i} \frac{z^i}{i!} \quad (32)$$

Here  $(x)_n$  is the Pochhammer symbol defined as

$$(x)_i = 1 \quad \text{for } i = 0$$

$$= x(x+1)\dots(x+i-1) \quad \text{for } i > 0 \quad (33)$$

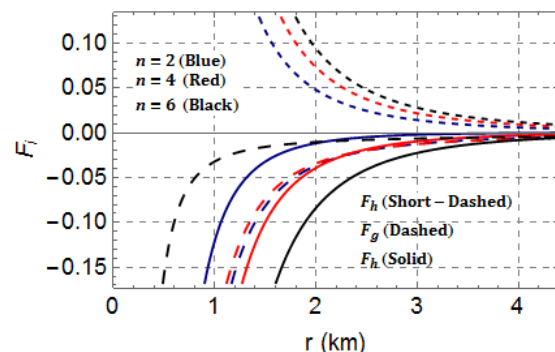


Figure 5. Variation of  $z_s$  and TOV-equation with radial coordinate  $r$  for  $c = 0.001, \alpha = 0.7, \beta = 0.001, \lambda = 101$  and  $k = 0.01$ .

On using (28) and (31) in (25)-(27) we can get expressions of all the physical parameters as

$$8\pi_F \rho(r) = \frac{2cn}{(cr^2 + \lambda)^{n+1}} + \frac{\lambda - (cr^2 + \lambda)^{-n}}{r^2} \quad (34)$$

$$8\pi_F p_r(r) = \alpha \left\{ 8\pi_F \rho(r) \right\} - 8\pi_F \beta \quad (35)$$

$$8\pi_F p_t(r) = \frac{(cr^2 + \lambda)^{-n-2}}{4r^2} X$$

$$\left[ c^2 r^4 \left\{ f_3(r) + f_4(r) + 2n f_5(r) \right\} + 2c\lambda r^2 \right.$$

$$\left. \left\{ f_6(r) + f_7(r) + n f_8(r) \right\} + \lambda^2 \left\{ f_1(r) + f_2(r) \right\} \right] \quad (36)$$

$$\Delta(r) = 8\pi_F (p_t - p_r) \quad (37)$$

The variations of all the above physical parameters are shown in Figure 1 and 2. The equation of state parameters  $\omega_r = p_r/\rho$  and  $\omega_t = p_t/\rho$  are always less than unity signifying these solutions can represent physically possible matters, see Figure 3.

Here

$$f_1(r) = 64\pi_F^2 \beta^2 r^4 (cr^2 + \lambda)^{2n} - 2\alpha \left\{ \lambda (cr^2 + \lambda)^n \right.$$

$$\left. - 1 \right\} \left\{ 8\pi_F \beta r^2 (cr^2 + \lambda)^n - \lambda (cr^2 + \lambda)^n \right.$$

$$\left. + 1 \right\} \quad (38)$$

$$f_2(r) = \alpha^2 \left\{ \lambda (cr^2 + \lambda)^n - 1 \right\}^2 - 16\pi_F \beta r^2$$

$$\left\{ \lambda (cr^2 + \lambda)^n + 1 \right\} (cr^2 + \lambda)^n$$

$$+ \left\{ \lambda (cr^2 + \lambda)^n - 1 \right\}^2 \quad (39)$$

$$f_3(r) = 1 - 16\pi_F \beta r^2 (cr^2 + \lambda)^n - 16\pi_F \beta \lambda r^2$$

$$(cr^2 + \lambda)^{2n} - 2\lambda (cr^2 + \lambda)^n + 64\pi_F^2 \beta^2 r^4$$

$$(cr^2 + \lambda)^{2n} + 4(\alpha - 1)\alpha n^2 \quad (40)$$

$$f_4(r) = \alpha^2 \left\{ \lambda (cr^2 + \lambda)^n - 1 \right\}^2 - 2\alpha \left\{ \lambda (cr^2 + \lambda)^n - 1 \right\}$$

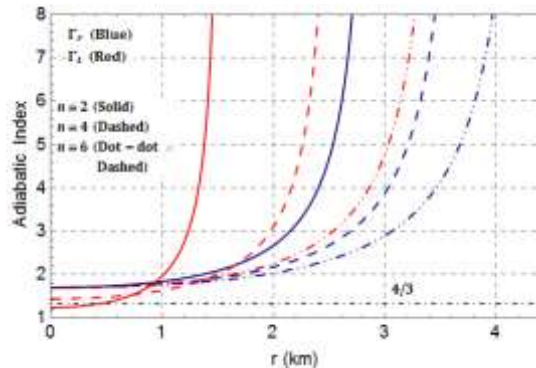
$$\left\{ 8\pi_F \beta r^2 (cr^2 + \lambda)^n - \lambda (cr^2 + \lambda)^n + 1 \right\} +$$

$$\lambda^2 (cr^2 + \lambda)^{2n} \quad (41)$$



$$f_5(r) = 2\alpha^2 \left\{ \lambda (cr^2 + \lambda)^n - 1 \right\}^2 + \alpha \left\{ -16\pi_F \beta r^2 \right. \\ \left. (cr^2 + \lambda)^n + 3\lambda (cr^2 + \lambda)^n - 1 \right\} - 8\pi_F \beta r^2 \\ (cr^2 + \lambda)^n + \lambda (cr^2 + \lambda)^n - 1 \quad (42)$$

$$f_6(r) = -16\pi_F \beta r^2 (cr^2 + \lambda)^n - 16\pi_F \beta \lambda r^2 \\ (cr^2 + \lambda)^{2n} - 2\lambda (cr^2 + \lambda)^n + 64\pi_F^2 \beta^2 r^4 \\ (cr^2 + \lambda)^{2n} + 1 \quad (43)$$



$$f_7(r) = \alpha^2 \left\{ \lambda (cr^2 + \lambda)^n - 1 \right\}^2 - 2\alpha \left\{ \lambda (cr^2 + \lambda)^n - 1 \right\} \\ \left\{ 8\pi_F \beta r^2 (cr^2 + \lambda)^n - \lambda (cr^2 + \lambda)^n + 1 \right\} + \\ \lambda^2 (cr^2 + \lambda)^{2n} \quad (44)$$

$$f_8(r) = 2\alpha^2 \left\{ \lambda (cr^2 + \lambda)^n - 1 \right\} + \alpha \left\{ -16\pi_F \beta r^2 \right. \\ \left. (cr^2 + \lambda)^n + 3\lambda (cr^2 + \lambda)^n \right\} - 8\pi_F \beta r^2 \\ (cr^2 + \lambda)^n + \lambda (cr^2 + \lambda)^n - 1 \quad (45)$$

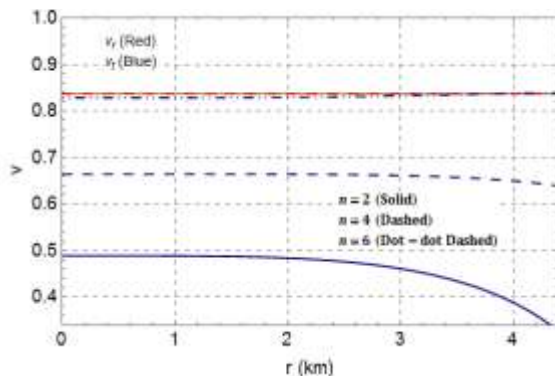


Figure 6. Variation of adiabatic index and speed of sound with radial coordinate  $r$  for  $c = 0.001, \alpha = 0.7, \beta = 0.001, \lambda = 101$  and  $k = 0.01$ .

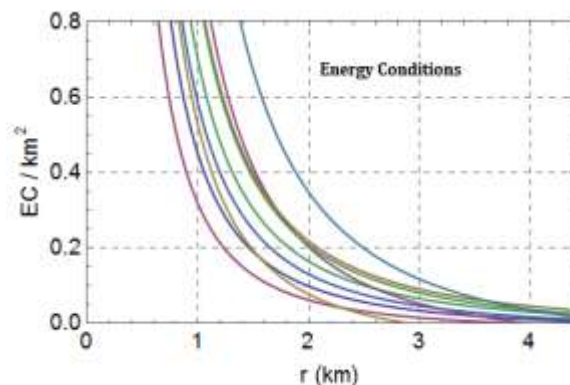
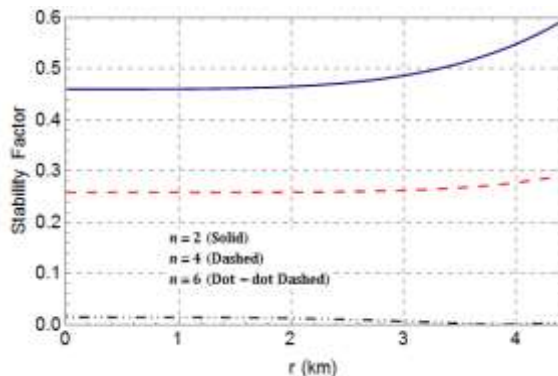


Figure 7. Variation of stability factor and energy conditions with radial coordinate  $r$  for  $c = 0.001, \alpha = 0.7, \beta = 0.001, \lambda = 101$  and  $k = 0.01$ .

The gradients of density and pressure can be written as

$$8\pi_F \frac{dp}{dr} = \frac{2}{r^3} \left[ (cr^2 + \lambda)^{-n-2} \left\{ -c^2(2n^2 + n \right. \right. \\ \left. \left. - 1)r^4 + c\lambda(n+2)r^2 + \lambda^2 \right\} - \lambda \right] \quad (46)$$

$$8\pi_F \frac{dp_r}{dr} = -\frac{2\alpha(cr^2 + \lambda)^{-n-2}}{r^3} \left[ c^2 r^4 \left\{ \lambda (cr^2 + \lambda)^n \right. \right. \\ \left. \left. + 2n^2 + n - 1 \right\} + \lambda^2 \left\{ \lambda (cr^2 + \lambda)^n - 1 \right\} \right. \\ \left. + c\lambda r^2 \left\{ 2\lambda (cr^2 + \lambda)^n - n - 2 \right\} \right] \quad (47)$$

and here we avoid to write the  $dp_t/dr$  due to its lengthy expression.

### Properties of the new model

This new solutions contains a singularity at the center where density and pressure are infinite i.e.

$$p_{rc} = p_{tc} = \infty \quad (48)$$

$$\rho_c = \infty \quad (49)$$

However,  $\omega_{rc} \equiv p_{rc}/\rho_c = \alpha$  and  $\omega_{tc} \equiv p_{tc}/\rho_c = (\alpha + 1)2(\lambda n + 1 - 1)/4$  are finite

at the center and thus Zeldovich's condition i.e.  $p_{rc}/\rho_c$  at centre should be  $\leq 1$ . Therefore,

$$\frac{p_{rc}}{\rho_c} = \alpha \leq 1 \quad (50)$$

Here we can see that the Zeldovich's condition  $\alpha \leq 1$  also imply the causality condition i.e.  $dp_r/d\rho = \alpha \leq 1$ . The condition  $\omega_{tc} > 0$  also requires  $\lambda$  to be greater than unity.

### Matching of physical boundary conditions

The exterior spacetime in Finslerian spacetime is given by Li & Chang (2014) as

$$F^2 = \left(1 - \frac{2M}{\lambda r}\right) y^t y^t - \left(\lambda - \frac{2M}{r}\right)^{-1} y^r y^r - r^2 \bar{F}^2(\theta, \phi, y^\theta y^\phi) \quad (51)$$

Table 1. Optimization of masses and radii of few well known compact star candidates.

Compact star	$c$	$\alpha$	$\beta$	$n$	Observed values		Calculated values		$u$	$z_s$
	(km <sup>-2</sup> )	(km <sup>-2</sup> )			$M/M_\odot$	$R(\text{km})$	$M/M_\odot$	$R(\text{km})$		
4U 1538-52	0.01073	0.23	0.001	2.2	$0.87 \pm 0.07$	$7.866 \pm 0.21$	0.871	7.86	7.86	0.222
0.752										
SMC X-4	0.00751	0.35	0.001	2.7	$1.29 \pm 0.05$	$8.831 \pm 0.09$	1.290	8.83	8.83	0.292
0.914										

$$B(r_b) = 1 - \frac{2M}{\lambda r_b} = \frac{k}{r_b^{\alpha+1}} (cr_b^2 + \lambda)^{\alpha n} \exp \left[ \frac{1}{2} (cr_b^2 + \lambda)^n \left\{ -\frac{8\pi_F \beta}{c(n+1)} [cr_b^2 + \lambda - \lambda \left( \frac{cr_b^2}{\lambda} + 1 \right)^{-n}] + \frac{(\alpha+1)\lambda}{n} \left( \frac{\lambda}{cr_b^2} + 1 \right)^{-n} \right\} \right] {}_2F_1 \left[ -n, -n; 1-n; -\frac{\lambda}{cr_b^2} \right] \quad (53)$$

$$P_r(r_b) = 0. \quad (54)$$

Using the boundary condition (52-54), we get

$$c = \frac{1}{r_b^2} \left[ \left( \lambda - \frac{2M}{r_b} \right)^{-1/n} - \lambda \right] \quad (55)$$

$$\beta = \frac{\alpha (cr_b^2 + \lambda)^{-n-1}}{8\pi_F r_b^2} \left[ \lambda^2 (cr_b^2 + \lambda)^n + c\lambda r_b^2 (cr_b^2 + \lambda)^n + 2cnr_b^2 - cr_b^2 - \lambda \right] \quad (56)$$

By matching the interior solution (10) and exterior solution (51) at the boundary  $r = r_b$  we obtain

$$A(r_b)^{-1} = \lambda - \frac{2M}{r_b} = (\lambda + cr_b^2)^{-n} \quad (52)$$

$$\ln k = \ln \left( 1 - \frac{2M}{\lambda r_b} \right) - \frac{1}{2} (cr_b^2 + \lambda)^n \left[ \frac{-8\pi_F \beta}{c(n+1)} \left\{ cr_b^2 + \lambda - \lambda \left( \frac{cr_b^2}{\lambda} + 1 \right)^{-n} \right\} + \frac{(\alpha+1)\lambda}{n} \right] {}_2F_1 \left[ -n, -n; 1-n; -\frac{\lambda}{r_b^2} \right] - \ln \left( \frac{(cr_b^2 + \lambda)^{\alpha n}}{r_b^{\alpha+1}} \right) \quad (57)$$

and we have chosen  $\lambda$ ,  $M$  and  $r_b$  as free parameters and the rest of the constants are determined from the Eqs. (55-57).

The mass-radius relation, compactness parameter and surface red-shift of the solution can be determined using the equation given below:

$$m(r) = 4\pi \int_0^r \rho r^2 dr = \frac{r}{2} \left[ \lambda - (cr^2 + \lambda)^{-n} \right] \quad (58)$$

$$u(r) = \frac{2m(r)}{r} = \lambda - (cr^2 + \lambda)^{-n} \quad (59)$$

$$z_s = \sqrt{\lambda A(r_b) - 1} \quad (60)$$

The variations of mass, compactness parameter and surface red-shift are shown in Figure 4 and 5



(left) respectively.

### Equilibrium and stability conditions condition for equilibrium

For a stellar system in equilibrium under different forces, the generalized Tolman-Oppenheimer-Volkoff (TOV) equation must be satisfied. The TOV equation in Finsler space-time was proposed by Varela *et al.* (2010) as

$$-\frac{M_g(\rho + p_r)}{r^2} \sqrt{\frac{A}{B}} - \frac{dp_r}{dr} + \frac{2\Delta}{r} = 0 \quad (61)$$

where  $M_g(r)$  is the effective gravitational mass contained within a sphere of radius  $r$  and is defined by the Tolman-Whittaker formula viz.,

$$M_g(r) = \frac{r^2}{2} \frac{B'}{\sqrt{AB}} \quad (62)$$

Equation (61) can be written in terms of balanced force equation due to anisotropy ( $F_a$ ), gravity ( $F_g$ ) and hydrostatic ( $F_h$ ) i.e.

$$F_g + F_h + F_a = 0 \quad (63)$$

Here

$$F_g = -\frac{B'}{2B}(\rho + p_r) \quad (64)$$

$$F_h = -\frac{dp_r}{dr} \quad (65)$$

$$F_a = \frac{2\Delta}{r} \quad (66)$$

The TOV equation (63) can be represented graphically showing the interplay amongst  $F_g$ ,  $F_h$  and  $F_a$  required to bring about equilibrium as evidenced in Figure 5 (right).

### Relativistic adiabatic index and stability

For a relativistic anisotropic sphere the stability is related to the adiabatic index  $\Gamma$ , the ratio of two specific heats, defined by Chan *et al.* (1993),

$$\Gamma_r = \frac{\rho + p_r}{p_r} \frac{dp_r}{dr}, \quad \Gamma_t = \frac{\rho + p_t}{p_t} \frac{dp_t}{dp} \quad (67)$$

Now  $\Gamma_r > 4/3$  gives the condition for the stability of a Newtonian sphere and  $\Gamma = 4/3$  being the condition for a neutral equilibrium proposed by Bondi (1964). This condition changes for a relativistic isotropic sphere due to the regenerative effect of pressure, which renders the sphere more unstable. For an anisotropic general relativistic sphere the situation becomes

more complicated, because the stability will depend on the type of anisotropy. For an anisotropic relativistic sphere the stability condition is given by Chan *et al.* (1993),

$$\Gamma_r > \frac{4}{3} + \left[ \frac{4}{3} \frac{p_{t0} - p_{r0}}{|p_{r0}|r} + \frac{8\pi}{3} \frac{\rho_0 p_{r0}}{|p_{r0}|} \right] \quad (68)$$

where,  $p_{r0}$ ,  $p_{t0}$ , and  $\rho_0$  are the initial radial, tangential, and energy density in static equilibrium satisfying (61). The first and last term inside the square brackets represent the anisotropic and relativistic corrections respectively and both the quantities are positive which increase the unstable range of  $\Gamma_r$  (Herrera *et al.* 1979; Chan *et al.* 1993). From the Figure 6 (left), it is clearly seen that  $\Gamma_r$  for these solutions is always more than the Newtonian fluids.

### Causality and stability condition

The radial and tangential speeds of sound of our compact star model are given by,

$$v_r^2 = \frac{dp_r}{d\rho} = \alpha, \quad v_t^2 = \frac{dp_t}{d\rho} = \frac{dp_t/dr}{d\rho/dr} \quad (69)$$

The profile of  $v_r^2$  and  $v_t^2$  are given in Figure 6 (right) which indicates that both the radial and transverse velocity satisfy the causality conditions i.e. both  $v_r^2$ ,  $v_t^2$  are less than 1 and monotonic decreasing function of  $r$  (Figure 6 right).

The stability of anisotropic stars under the radial perturbations is studied by using the concept of Herrera (1992) known as Herrera's "cracking" method. Using the concept of cracking, Abreu (1992) showed that the region of the anisotropic fluid sphere where  $0 \leq |v_t^2 - v_r^2| \leq 1$  (see Figure 7 left) is a stable configuration.

### Results and Discussions

We have successfully explored a family of new exact solutions by assuming a particular form of metric coefficient in the background of MIT-bag EoS. These new solutions can describe bounded configurations which are anisotropic in pressure. These solutions are regular and well behaved except at the center. Since the EoS parameters are less than unity, these solutions describe a physically possible fluid distributions. This very result is also supported further due to the solution satisfies all the energy conditions. Since the speed of sound at the interior are less than unity, these solutions obey causality condition. Modelling of static and stable bounded configurations are also possible since these solutions also satisfies the static and

stability conditions i.e.  $0 \leq |v_t^2 - v_r^2| \leq 1$  and  $\Gamma_r > 4/3$ . An interesting property of these solutions is that the Zeldovich's condition directly imply the causality condition since  $v_r^2 = \alpha$ . On the other hand, the stellar configurations described by these solutions are solely depends on parameter  $n$ . For small values of  $n$  corresponds to softer EoSs that yields less massive and smaller configurations however, larger values of  $n$  gives more denser, massive and bigger configurations where the EoSs are stiffer. It is also observed that

the anisotropy is more for smaller values of  $n$ . Indeed, the central values of compactness parameter and surface red-shift are non-zero since the metric potential  $A(r)$  is not unity at  $r = 0$  which was needed to be unity in Einstein's gravity. Finally, we present two models of compact stars in Table 1, 4U 153852 and SMC X-4 where the observed masses and radii are well fitted with the calculated values from the presented solutions (Gangopadhyay *et al.* 2013).

## References:

1. Abreu H, Hernández H, Núñez L A 2007. Sound speeds, cracking and the stability of self-gravitating anisotropic compact objects. *Class. Quantum Grav.* 24:4631-4645.
2. Akbar-Zadeh H 1988. Sur les espaces de Finsler à courbures sectionnelles constants. *Acad. R. Belg. Bull. Cl. Sci.* 74:281-322.
3. Bao D, Chern, S -S, Shen Z 2000. *An Introduction to Riemann Finsler geometry* (Springer, New York).
4. Bhar P 2015a. Singularity-free anisotropic strange quintessence star. *Astrophys. Space Sci.* 356:309-318.
5. Bhar P 2015b. A new hybrid star model in Krori-Barua spacetime. *Astrophys. Space Sci.* 357:46.
6. Bhar P, Govender M, Sharma R 2017. A comparative study between EGB gravity and GTR by modeling compact stars. *Eur. Phys. J. C.* 77:109.
7. Bohmer C G, Harko T, Lobo F S N 2008. Dark matter as a geometric effect in  $f(R)$  gravity. *Astroparticle Phys.* 29:386-392.
8. Bondi H 1964. The contraction of gravitating spheres. *Proc. R. Soc. Lond. Ser. A* 281:39-48.
9. Capozziello, S, De Laurentis M, Odintsov S D, Stabile A 2011. Hydrostatic equilibrium and stellar structure in  $f(R)$  gravity. *Phys. Rev. D.* 83:064004.
10. Capozziello S, De Laurentis M, De Martino I, Formisano M, Odintsov S D 2012. Jeans analysis of self-gravitating systems in  $f(R)$  gravity. *Phys. Rev. D.* 85:044022.
11. Cartan E 1934. Les Espaces de Finsler. *Actualite Scientifiqueset Industrielles.* 79:40.
12. Chan R, Herrera L, Santos N O 1993. Dynamical instability for radiating anisotropic collapse. *Mon. Not. R. Astron. Soc.* 265:533-544
13. Dadhich N, Molina A, Khugaev A 2010. Uniform density static fluid sphere in Einstein-Gauss-Bonnet gravity and its universality. *Phys. Rev. D.* 81:104026.
14. Dadhich N, Pons J M, Prabhu K 2013. On the static Lovelock black holes. *Gen. Relativ. Gravit.* 45:1131-1144.
15. Delgaty M S R, Lake K 1998. Physical acceptability of isolated, static, spherically symmetric, perfect fluid solutions of Einstein's equations. *Comp. Phys. Commun.* 115:395-415.
16. Gangopadhyay T, Ray R, Li Z-D, Dey J, Dey M 2013. Strange star equation of state fits the refined mass measurement of 12 pulsars and predicts their radii. *Mon. Not. R. Astron. Soc.* 431:3216-3221.
17. Ghosh S G, Deshkar D W 2008. Horizons of radiating black holes in Einstein-Gauss-Bonnet gravity. *Phys. Rev. D.* 77:047504.
18. Herrera L, Ruggeri G J, Witten L 1979. Adiabatic contraction of anisotropic spheres in general relativity. *Astrophys. J.* 234:1094-1099.
19. Herrera L 1992. Cracking of self-gravitating compact objects. *Phys. Lett. A.* 165, 206-210.
20. Horvath J I 1950. A geometrical model for the unified theory of physical fields. *Phys. Rev. D.* 80:901.
21. Jhingan S, Ghosh S G 2010. Inhomogeneous dust collapse in 5D Einstein-Gauss-Bonnet gravity. *Phys. Rev. D.* 81:024010.
22. Li X, Chang Z 2014. Exact solution of vacuum field equation in Finsler spacetime. *Phys. Rev. D.* 90:064049.
23. Lovelock D 1971. The Einstein tensor and its generalizations. *J. Math. Phys.* 12:498-501.
24. Lovelock D 1972. The Four-Dimensionality of Space and the Einstein Tensor. *J. Math. Phys.* 13:874-876.
25. Rajpoot S, Vacaru S 2015. Black ring and Kerr ellipsoid-Solitonic configurations in modified Finsler gravity. *Int. J. Geom. Meth. Mod. Phys.* 12:1550102.
26. Rahaman F, Paul N, De S S, Ray S, Jafry Md A K 2015. The Finslerian compact star model. *Eur. Phys. J. C.* 75:564.
27. Rahaman F, Paul N, Banerjee A, De S. S., Ray S, Usmani A. A. 2016. The Finslerian wormhole models. *Eur. Phys. J. C.* 76:246.
28. Schreck M 2015. Classical kinematics and Finsler structures for nonminimal Lorentz-violating fermions. *Eur. Phys. J. C.* 75:187.
29. Singh K N, Pradhan N, Pant N 2015. Charge Analogue of Tolman IV Solution for Anisotropic Fluid. *Int. J. Theor. Phys.* 54:3408- 3423.
30. Singh K N, Pant N 2015a. Charged anisotropic superdense stars with constant stability factor. *Astrophys. Space Sci.* 358:44.
31. Stavrinou P, Vacaru S 2013. Cyclic and ekpyrotic universes in modified Finsler osculating gravity on tangent Lorentz bundles. *Class. Quant. Gravit.* 30:055012.
32. Stelle K S 1977. Renormalization of higher-derivative quantum gravity. *Phys. Rev. D.* 16:953.
33. Utiyama R, DeWitt B S 1962. Renormalization of a Classical Gravitational Field Interacting with Quantized Matter Fields. *Math. Phys.* 3:608.
34. Vacaru S 2010. Critical remarks on Finsler modifications of gravity and cosmology by Zhe Chang and Xin Li. *Phys. Lett. B* 690:224-228.
35. Vacaru S 2012. Principles of Einstein-Finsler gravity and perspectives in modern cosmology. *Int. J. Mod. Phys. D.* 21:1250072.

36. Vacaru S 1997. Superstrings in higher order extensions of Finsler superspaces. *Nucl. Phys. B.* 434:590-656.
37. Vacaru S 1996. [Spinor structures and nonlinear connections in vector bundles, generalized Lagrange and Finsler spaces.](#) *J. Math. Phys.* 37:508.
38. Vacaru S 2012. Modified dispersion relations in Hořava–Lifshitz gravity and Finsler brane models. *Gen. Relat. Gravit.* 44:1015-1042.
39. Varela V, Rahaman F, Ray S, Chakraborty K, Kalam M 2010. Charged anisotropic matter with linear or nonlinear equation of state. *Phys. Rev. D.* 82:044052.
40. Woodard R P 2007. The invisible universe: Dark matter and dark energy. *Lect. Notes Phys.* 720:403.
41. Zubair M, Abbas G 2016. Some interior models of compact stars in  $f(R)$  gravity. *Astrophys. Space Sci.* 361:342.

Please cite this article as: Ksh. Newton Singh, M. V. Mandke, Anil K. Aria (2021). A family of Finslerian space-time obeying MIT-bag equation of state . *International Journal of Recent Research and Applied Studies*, 8, 4(1), 1-12.